Modeling the Adsorption of Metal–EDTA Complexes onto Oxides

ARTICLE *in* ENVIRONMENTAL SCIENCE & TECHNOLOGY · JUNE 1996

Impact Factor: 5.33 · DOI: 10.1021/es9508939

4 AUTHORS:

Bernd Nowack
Empa - Swiss Federal Laboratories for Materi…
180 PUBLICATIONS **9,414** CITATIONS
SEE PROFILE

Johannes Lützenkirchen
Karlsruhe Institute of Technology
117 PUBLICATIONS **1,315** CITATIONS
SEE PROFILE

Philippe Behra
Institut National Polytechnique de Toulouse
63 PUBLICATIONS **1,378** CITATIONS
SEE PROFILE

Laura Sigg
Eawag: Das Wasserforschungs-Institut des E…
159 PUBLICATIONS **7,620** CITATIONS
SEE PROFILE

Environ. Sci. Technol. **1996**, *30,* 2397−2405

Modeling the Adsorption of Metal−EDTA Complexes onto Oxides

BERND NOWACK,[†,§] JOHANNES LÜTZENKIRCHEN,[‡] PHILIPPE BEHRA,[‡] AND LAURA SIGG*[,†]

Swiss Federal Institute for Environmental Science and Technology (EAWAG) and Swiss Federal Institute of Technology (ETH), CH-8600 Dübendorf, Switzerland, and Institut de Mécanique des Fluides de l'Université Louis Pasteur, URA CNRS 854, 2 rue Boussingault, F- 67000 Strasbourg, France

The adsorption of metal−EDTA complexes onto various oxides (aluminium oxides, crystalline and amorphous iron oxides) was described by the surface complexation model. Data from the literature and from our experiments with several oxides were analyzed by assuming only one type of ternary surface complex for Me^{2+}−EDTA complexes. The surface complexes exhibit an anionic character with decreasing adsorption with increasing pH. This proposed model allows us to describe all available data sets very well. The adsorption of NiEDTA was interpreted by several models (constant capacitance, diffuse layer) onto different oxides (with different pK_a values). Log K values within one model agree very well with each other. The pH, where 50% of the complex is adsorbed, increases in the series HFO < lepidocrocite < γ-Al_2O_3 < goethite < δ-Al_2O_3 from 6.5 to 8.35 (for 1 μM NiEDTA and 1 mM surface groups). Adsorption of Fe(III)EDTA onto several oxides was studied. Two types of surface complexes, anionic and cationic, were necessary to explain the observed adsorption edge. Fe(III)EDTA is adsorbed over a wide pH range and is the major adsorbed EDTA species at pH greater than 7.

Introduction

Chelating agents can significantly influence the migration behavior of toxic metals like Pb, Cd, or radioactive compounds in soils, sediments, and aquifer systems. The mobility of trace metals is of special interest because of the possibility of bioaccumulation and health risks. Although metals may be strongly adsorbed onto soils and aquifer materials such as clays and oxides, such association does not guarantee long-term immobilization of contaminant metals in the subsurface environment. Enhanced transport of metal ions in the presence of organic ligands has been observed (*1*) because of the difference in sorption behavior between the anionic complex and the free metal (*2*).

Ethylenediaminetetraacetic acid (EDTA) is one of the most widely used industrial complexing agents (photographic industry, textile and paper manufacturing, industrial cleaning). In effluents from wastewater treatment plants, concentrations up to 18 μM have been reported due to its low biodegradability (*3*). After discharge, it persists as a major pollutant in rivers (*4*, *5*), lakes (*6*, *7*), and groundwaters (*8*). For rivers, concentrations up to 0.6 μM are reported with typical concentrations between 10 and 100 nM (*4*, *5*). A concentration of 31.4 mM was found in the Hanford site (*9*), where EDTA among other complexing agents was used to decontaminate radioactive equipment from the nuclear industry. The waste, containing both complexing agents and radioactive metals like ^{60}Co, was dumped into the ground, where the anionic complexes persist even years later.

Surface reactions of uncomplexed EDTA with iron and aluminium oxides have been studied extensively (*10*−*12*). However, chelating agents like EDTA are present in natural systems generally as metal complexes, mainly as Fe(III)-EDTA, CaEDTA, and ZnEDTA (*13*). Adsorption of metal−EDTA complexes to iron and aluminium oxides has been studied by several authors (*2*, *14*−*17*).

Adsorption is also a key factor in the dissolution of oxides by ligands or in the inhibition of dissolution. Dissolution rates have been shown to be linear functions of the surface concentration of the ligand (*18*, *19*). Knowledge of the adsorption behavior of metal−ligand complexes in model systems may enable better predictions of their behavior in natural systems. However, a clear distinction between adsorption and dissolution reactions is often difficult to observe under conditions where oxide dissolution is fast (*20*). The formation of Fe(III)EDTA may change the adsorption behavior of EDTA in the system due to the occurrence of other surface species. It was shown for goethite (*16*) that the maximum adsorption capacity of Fe(III)EDTA is about 80 times less than that of other metal−EDTA species (e.g., ZnEDTA).

The speciation of EDTA, therefore, has a strong influence on its fate in natural systems. The influence of speciation on the behavior of EDTA in sewage treatment plants and rivers has been investigated (*3*−*5*). The fraction of FeEDTA is of special interest because it can be totally photolyzed in a river on a sunny day within several hours (*4*). FeEDTA is either released by industry as a complex or is formed in sewage treatment plants with phosphate precipitation by iron salts. In the effluents, the fraction of FeEDTA of total EDTA is between 20 and 90% (*3*). In a river in the vicinity of a sewage treatment plant, high concentrations of FeEDTA are possible, which are rapidly depleted by sunlight. Calculations showed that FeEDTA is not at equilibrium in waters with high calcium concentrations and pH values between 7 and 8. But the exchange reactions of FeEDTA with other metals like Zn or Ca are slow (*13*) and do not significantly influence EDTA speciation. Other metal−EDTA complexes are degraded by light only to a minor

* Corresponding author telephone: +41-1-8235494; fax: +41-1-8235028; e-mail address: sigg@eawag.ch.

† EAWAG and ETH.

§ Present address: Swiss Federal Laboratory for Materials Testing and Research (EMPA), CH-9001 St. Gallen, Switzerland.

‡ Institut de Mécanique des Fluides de l'Université Louis Pasteur.

S0013-936X(95)00893-5 CCC: $12.00

extent [Mn(II)EDTA, Co(III)EDTA] or are insensitive toward light (*5*).

A source of Fe(III)EDTA in aquifers is the infiltration of river waters. Fe(III)EDTA can also be formed by dissolution reactions of metal−EDTA complexes with iron oxides below pH 6−7 (*1*, *2*).

The purpose of this paper is to describe the available experimental data on the adsorption of different metal−EDTA complexes to oxides by the same model to allow comparison. Intrinsic, pH-independent equilibrium constants are obtained for different data sets. All data are explained by the surface complexation model with preferentially one unique surface reaction. For Fe(III)EDTA, we had to include several surface complexes into the model [similar to Dzombak and Morel (*21*) for the adsorption of anions to hydrous ferric oxide (HFO)]. Experiments were done with a variety of oxides (crystalline and amorphous iron oxides, aluminium oxide) and with three metal−EDTA complexes [NiEDTA, PdEDTA, and Fe(III)EDTA]. Special attention was paid to the adsorption of Fe(III)EDTA to oxides because this species may be prevalent in natural systems.

Methods

Nanopure water (>18 MΩ) was obtained from a Barnstead Nanopure apparatus. All chemicals were analytical grade, purchased from Merck or Fluka, except for HNO_3, NaOH, and $NaNO_3$, which were Merck Suprapur quality. All experiments were done with 0.01 M $NaNO_3$ as the background electrolyte at ambient CO_2 concentration and room temperature (22−24 °C). pH was measured with a Metrohm pH-meter and a Metrohm glass electrode, calibrated with standard buffers. Stock solutions (0.01 M) of metal−EDTA solutions were prepared by dissolving the metal−nitrate and $Na_2H_2EDTA{\cdot}2H_2O$ in water and boiling for 1 h. Fe(III)-EDTA was prepared by dissolving $NaFeEDTA{\cdot}2H_2O$ in water.

Preparation and Characterization of the Oxides. The goethite was synthesized according to Schwertmann and Cornell (*22*) and characterized as described in Nowack and Sigg (*16*). The lepidocrocite was synthesized as described in Karametaxas et al. (*23*). HFO (hydrous ferric oxide or ferrihydrite) was synthesised by rapid hydrolysis of an acidic 0.001 M $Fe(NO_3)_3$ solution with NaOH (no exclusion of CO_2). The suspension had an ionic strength of 0.01 M $NaNO_3$ and was aged at pH 7.5 ± 0.5 at room temperature for 16−20 h before use. Acid−base titrations were performed in solutions where CO_2 was removed by nitrogen. δ-Al_2O_3 (Degussa) was used without further purification. Its properties are described in Ochs (*24*).

Adsorption Experiments. For experiments with goethite or lepidocrocite, the oxide suspension, $NaNO_3$, and water were added to 50-mL polyethylene (PE) bottles. The pH was adjusted with different buffers: for pH 3−4.5, HNO_3 was used; for pH 5.2−6.8, MES (2-morpholinoethanesulfonic acid) buffer (2×10^{-3} M) and NaOH were used; for pH 6.8−8.2, HEPES [4-(2-hydroxyethyl)-1-piperazineethanesulfonic acid] (2×10^{-3} M) and NaOH were used; for pH >8.4, NaOH was used. HEPES (*25*, *26*) and MES (*26*) were found to have very weak complexing properties. Preliminary experiments showed that MES and HEPES did not influence the adsorption of EDTA species to goethite. The suspension was equilibrated at the desired pH value for 1 h before the addition of MeEDTA. Equilibration time was 30 min for NiEDTA and PdEDTA and 3 h for Fe(III)EDTA. These periods were found to be sufficient for adsorption. After 2 min, no change in the amount of adsorption was detected for EDTA and PbEDTA on goethite. Samples were withdrawn via a PE syringe, filtered through a 0.2-μm cellulose nitrate filter (Sartorius), and analyzed for EDTA. Adsorbed concentrations were calculated as the difference between the known total and the measured dissolved concentrations.

For adsorption experiments with HFO, the suspension was used without further treatment after aging. After the aging, the same buffers as described above were added, and the suspension was equilibrated for 1 h before the addition of EDTA. A filtration cutoff of 0.2 μm was sufficient to remove all oxide and was checked by measuring the iron concentration in the filtrate.

Adsorption experiments as a function of pH at constant MeEDTA concentration [5×10^{-7} M MeEDTA, 0.4 g/L oxide (goethite or lepidocrocite), or 0.08 g/L HFO] and as a function of MeEDTA concentration at constant pH (pH 3.5 and 5.5) and constant solid concentration were performed.

Analysis of EDTA. EDTA concentrations were determined by HPLC (*16*). The different metal−EDTA complexes were exchanged with $Fe(NO_3)_3$ to form Fe(III)EDTA, which was subsequently separated and specifically detected by UV absorption, as follows: 1-mL samples were evaporated to dryness in an oven at 70−90 °C. The residues were dissolved in 1 mL of formate buffer. A Fe(III) solution was added, and the solution was heated to 90 °C in a water bath for 1 h (3 h for NiEDTA experiments). The solution was then cooled to room temperature, tetrabutylammonium bromide solution (TBA-Br) was added, and the sample was pipetted into autosampler vials. The Fe(III)EDTA complex was separated on a Lichrocard 250-4 C_{18} column with a formate buffer eluent (0.001 M TBA-Br, 0.005 M sodium formate, 0.015 M formic acid, and 8% acetonitrile, pH 3.3). Detection was made by UV at 258 nm.

The PdEDTA complex was detected after complexation with Bi(III). In contrast to PdEDTA, Bi(III)EDTA can be detected at 258 nm. Instead of the Fe(III) addition, $BiCl_3$ solution was added. The rest of the procedure was the same as described above.

FITEQL. The adsorption parameters were determined using FITEQL2 (*27*). Experimental data from titrations included $TOTH^+$ (total proton concentration), TOTi (total analytical concentration of i), and log([H^+]/M) (logarithm of the free proton concentration). Activity coefficients were taken from Dzombak and Morel (*21*) when necessary. Error estimates for the experimental data for $TOTH^+$ were 0.01 (relative error) and 1×10^{-8} M (absolute error), and for log([H^+]/M) we used 0.04 and 0.0 as relative and absolute error, respectively (*28*). For the evaluation of the adsorption of MeEDTA, we used $MeEDTA_{ads}$ as a type II component (the free concentration of this component was set to unity). The relative error was 0.01, the absolute 0.01TOTMeEDTA (*10*). For our experimental data, we used 0.05 for the relative and 0.05TOTMeEDTA for the absolute error. The error for the free proton concentration was fixed as described above. The values for the relative error of log([H^+]/M) was modified for the FITEQL input as indicated in the manual.

An indication of the goodness of fit is the overall variance SOS/DF (weighted sum of squares/degrees of freedom). Values between 0.1 and 20 indicate a reasonably good fit (*21*). The standard deviation of log *K* values also depends on the error estimates of the experimental data.

Data Sets. The source of data sets from the literature are shown in Table 1. Acidity and adsorption constants were used when available. Otherwise, experimental data,

TABLE 1

Data Sets for Adsorption of Metal−EDTA Species onto Oxides Used in This Study

oxide	metal−EDTA species	data set	ref
HFO	Fe(III), Ni, Co(III), Pd		this study
lepidocrocite	Fe(III), Ni		this study
δ-Al_2O_3	Ni, Fe(III)		this study
goethite	Zn, Cu, Pb, Ni, Co(II), Pd, Co(III), Fe(III), Al(III)	Table 3	16
HFO	Ni	Table 2	14
δ-Al_2O_3	Co(II), Co(III), Al(III)	Figures 2−4	17
γ-Al_2O_3	Ni	Figure 45	10
γ-Al_2O_3	Zn, Cu, Cd, Pb, Ca, Ni	Figure 3a	15

typically pH-edge data, were extracted and analyzed. Experimental data were obtained for the oxides HFO, goethite, lepidocrocite, and δ-Al_2O_3.

Results

Characterization of the Oxides. The surface chemical properties of the oxides are summarized in Table 2, including BET surface (N_2 adsorption), concentration of adsorption sites, and pK_a values. To be able to compare the results to the literature, we decided to use the average surface area for HFO of Dzombak and Morel (*21*) of 600 m^2/g and the average number of surface sites of 0.205 mol/mol Fe. Both parameters depend strongly on the method by which they were measured. The average values of Dzombak and Morel (*21*) may, therefore, be more accurate than the experimental values. The titration data of the HFO were fitted to both constant capacitance (cc) and diffuse layer (dl) models, all the others just to the cc model. The titration of the HFO prepared in our laboratory gave a point of zero charge (pzc), which is more than 1 pH unit lower than the average value from the HFO database (*21*). This is possibly due to the presence of CO_2 during the formation of our HFO, which could alter the chemical properties of the oxide surface (during the titrations the CO_2 was excluded). Kanungo (*29*), on the other hand, has reported pzc values of 7.15 and 6.5 for HFO, which are in the same range as for our HFO. Iron(III) (hydr)oxides in natural systems are always formed in the presence of CO_2. Thus, while our HFO may not be comparable to those in the literature, it may better represent a naturally occurring HFO.

Formation of Ternary Surface Complexes. It has already been shown that metal−EDTA species adsorb as ternary surface complexes in a 1:1 metal to EDTA ratio (*14*, *16*, *17*). For several EDTA complexes [PbEDTA, Co(II)EDTA, NiEDTA], it was shown that both metal and EDTA were simultaneously adsorbed. Weak complexes like CaEDTA dissociate at low pH, and adsorption of both CaEDTA and uncomplexed EDTA has been found (*16*). In this paper, we always assume that a 1:1 complex has been formed.

The general description of the surface reaction for the EDTA complex of a divalent metal is

$$\equiv SOH + Me^{2+} + L^{4-} + H^+ \leftrightarrow \equiv S{-}L{-}Me^- + H_2O \qquad \log K_1 \quad (1)$$

or

$$\equiv SOH + MeL^{2-} + H^+ \leftrightarrow \equiv S{-}L{-}Me^- + H_2O \qquad \log K_2 \quad (2)$$

where ≡SOH represents a surface site, and L represents EDTA.

The two constants from eqs 1 and 2 can be related as follows:

$$\log K_2 = \log K_1 - \log K_{MeL} \quad (3)$$

where log K_{MeL} is the complexation stability constant in aqueous solution. The maximum adsorption capacity Γ_{max} was obtained by linearization of the adsorption isotherm at constant pH assuming a Langmuir-type behavior:

$$\{L_{ads}\} = \frac{\Gamma_{max} K_{ads}[L]}{1 + K_{ads}[L]} \quad (4)$$

where $\{L_{ads}\}$ is the total surface concentration of MeEDTA, and [L] is the total dissolved MeEDTA concentration.

Linearization was done according to Van den Berg and Kramer (*30*), which gives values for Γ_{max} that are more precise than the values by the Scatchard plot. Due to the much smaller surface coverage of the EDTA complexes compared to the protons, adsorption of metal−EDTA was considered to take place on specific surface sites (≡$FeOH_{spec}$) comprising a much smaller concentration than the sites that are available for protons:

$$\equiv FeOH_{spec} + \equiv FeOH_{unspec} = \equiv FeOH_{tot} \quad (5)$$

The concentration of ≡$FeOH_{spec}$ was estimated from Γ_{max} of the adsorption isotherm. For ≡$FeOH_{spec}$ and ≡$FeOH_{unspec}$, the same pK_a values as determined by acid−base titration were used [Dzombak and Morel (*21*) for weak and strong sites]. All calculations by the surface complexation model were done considering eq 5.

Adsorption of NiEDTA. The concentration of surface sites and the conditional log K_{ads} values for the adsorption of NiEDTA to different oxides are given in Table 3. If the maximum adsorption capacity is related to the surface area, Γ_{max} for NiEDTA is about the same for HFO (9.93×10^{-7} mol/m^2) and lepidocrocite (8.17×10^{-7} mol/m^2) whereas for goethite it is about twice as high. For HFO, the value of 0.053 mol sites/mol Fe for NiEDTA is close to values reported for the adsorption of metals like Hg(II) (*31*). In Figure 1, experimental data and model fits are shown for the adsorption isotherms for the three oxides HFO, goethite, and lepidocrocite.

Both adsorption isotherms at constant pH and adsorption edges were fitted according to the surface complexation model. Table 4 summarizes the estimated log K values for the adsorption of NiEDTA onto various oxides (according to eq 2). Using the electric double-layer model, the log K values obtained from different experimental setups for a given oxide differ by less than 0.5. The constants for different oxides vary due to the different pzc of the oxides. If our data of the adsorption of NiEDTA to HFO are fitted using the pK_a values for HFO from Dzombak and Morel (*21*), the log K for the adsorption of NiEDTA (8.44) is very close to the log K of 8.38 determined by Bryce et al. (*14*) for another HFO, but for the same pK_a values from ref 21. In Figure 2, measured and fitted adsorption edges are shown for HFO, goethite, and lepidocrocite. The assumption of one surface species is sufficient to explain the data available for the oxides very well. The adsorption isotherms at pH 5.5 were also fitted by the surface complexation model (Figure 1). The adsorption isotherm on HFO at pH 3.3 is very sensitive toward the total amount of specific surface sites ≡$FeOH_{spec}$ and was not considered. The constants obtained from the pH edge (pH 5−8) do not allow the

TABLE 2

Properties of Oxides Used in This Study, All Constants for $I = 0$ M

oxide	BET surface (m^2/g)	surface sites (μmol/m^2)	pK_{a1}	pK_{a2}	pzc	capacitance	model[a]	ref
HFO	600 (267)[b]	3.75[c]	6.09	7.38	6.74		dl	this study
HFO	600 (267)	3.75	5.08	8.09	6.59	0.8	cc	this study
HFO	600	3.75	7.29	8.93	8.11		dl	21
goethite	21	3.79	5.67	8.97	7.32	4.0	cc	16
lepidocrocite	78[d]	1.40	4.85	8.11	6.48	0.8	cc	this study
δ-Al_2O_3	100	3.20	5.83	8.77	7.30	4.0	cc	24
γ-Al_2O_3	100	1.60	6.94	8.59	7.77	2.8	cc	this study[e]

[a] cc, constant capacitance; dl, diffuse layer. [b] 267 were measured by BET; the value of 600 was taken from Dzombak and Morel (21); the calculations were done with this value. [c] 0.205 mol/mol of Fe, from Dzombak and Morel (*21*). [d] From Karametaxas et al. (*23*). [e] Values estimated from the titration data of Kehrer (*28*).

TABLE 3

Linearization of Adsorption Isotherms according to Van den Berg and Kramer (*30*)

oxide	species	Γ_{max} (mol/g)	Γ_{max}[a] (mol/mol of Fe)	Γ_{max} (mol/m^2)	log K_{ads}	pH
goethite	FeEDTA	8.95×10^{-7}		4.26×10^{-8}	6.47	3.3
HFO	FeEDTA	2.69×10^{-4}	0.024	4.48×10^{-7}	5.88	3.3
HFO	FeEDTA	1.86×10^{-4}	0.017	3.10×10^{-7}	5.57	5.4
HFO	FeEDTA	1.24×10^{-4}	0.011	2.07×10^{-7}	5.05	7.5
lepidocrocite	FeEDTA	3.67×10^{-6}		4.12×10^{-8}	5.91	3.3
goethite	NiEDTA	4.22×10^{-5}		2.01×10^{-6}	5.82	3.3
HFO	NiEDTA	5.96×10^{-4}	0.053	9.93×10^{-7}	6.22	3.3
HFO	NiEDTA	3.15×10^{-4}	0.028	5.25×10^{-7}	5.32	5.4
lepidocrocite	NiEDTA	7.27×10^{-5}		8.17×10^{-7}	5.21	3.3

[a] The molecular weight of HFO was assumed to be 89 g of HFO/mol of Fe (*21*).

TABLE 4

Intrinsic Log K Values for Adsorption of NiEDTA to Oxides ($I = 0$ M) for Reaction $\equiv SOH + L^{2-} + H^+ \leftrightarrow \equiv S{-}L{-}Ni^- + H_2O$

oxide	ref	log K	model	ratio EDTA:surface sites	error estimate SOS/DF	experiment[a]
HFO	this study	9.36 ± 0.1	cc	415	0.81	pH edge
HFO	this study	9.66 ± 0.05	cc	10−2	1.09	a.i. at pH 5.5
HFO	this study	9.29 ± 0.10	dl	415	1.07	pH edge
HFO	this study	8.99 ± 0.05	dl	10−2	0.42	a.i. at pH 5.5
HFO	this study[b]	8.62 ± 0.10	dl	415	1.05	pH edge HFO
HFO	this study[b]	8.12 ± 0.05	dl	10−2	1.46	a.i. at pH 5.5
HFO	14[b]	8.38	dl	184		pH edge
goethite	16	11.26 ± 0.03	cc	78	2.73	pH edge
goethite	16	11.18 ± 0.05	cc	28−2	12.86	a.i. at pH 3.3
lepidocrocite	this study	10.42 ± 0.04	cc	122	6.65	pH edge
lepidocrocite	this study	10.30 ± 0.09	cc	7−0.5	99.3	a.i. at pH 3.3
δ-Al_2O_3	this study	11.55 ± 0.11	cc	320	0.43	pH edge
γ-Al_2O_3	15	10.44	cc	16	0.11	pH edge

[a] a.i., adsorption isotherm. [b] Calculated with the pK_a values from Dzombak and Morel (*21*).

prediction of the adsorption at pH 3.3; they are only valid in the concentration and pH range where they were determined.

For HFO, both models, the Langmuir model and the surface complexation model (SCM), agree very well, though the SCM is able to describe the system slightly better (Figure 1). For goethite and lepidocrocite, more significant differences were found between Langmuir and SCM.

Figures 3 and 4 show the pH-adsorption edges for NiEDTA onto γ-Al_2O_3 for data from Bowers (*10*) and to δ-Al_2O_3 for own experimental data, respectively. In both cases the observed pH edge is well described by a single surface complex model.

Because the different oxides have different pK_a values, the calculated adsorption constants cannot be directly compared. However, we can calculate the pH of 50% adsorption (pH_{50}) for the same MeEDTA concentration and surface site concentration present in the aqueous phase for all oxides (10^{-6} M MeEDTA, 1 mM surface sites). Under these identical conditions, we can compare the adsorption affinity to different oxides. Table 5 shows the pH_{50} values for different oxides and complexes. The pH_{50} varies between 6.5 and 6.6 for the HFO of this study and that of Bryce et al. (*14*), respectively, and 8.4 for the δ-Al_2O_3 of this study. Goethite, γ-Al_2O_3, and lepidocrocite have a pH_{50} of 8.1, 7.5, and 7.3, respectively. The adsorption, normalized to the amount of surface sites, is therefore strongest for aluminum oxides followed by goethite, lepidocrocite, and then HFO. In Figure 5, the calculated adsorption edges using identical conditions (1×10^{-6} M NiEDTA, 1 mM

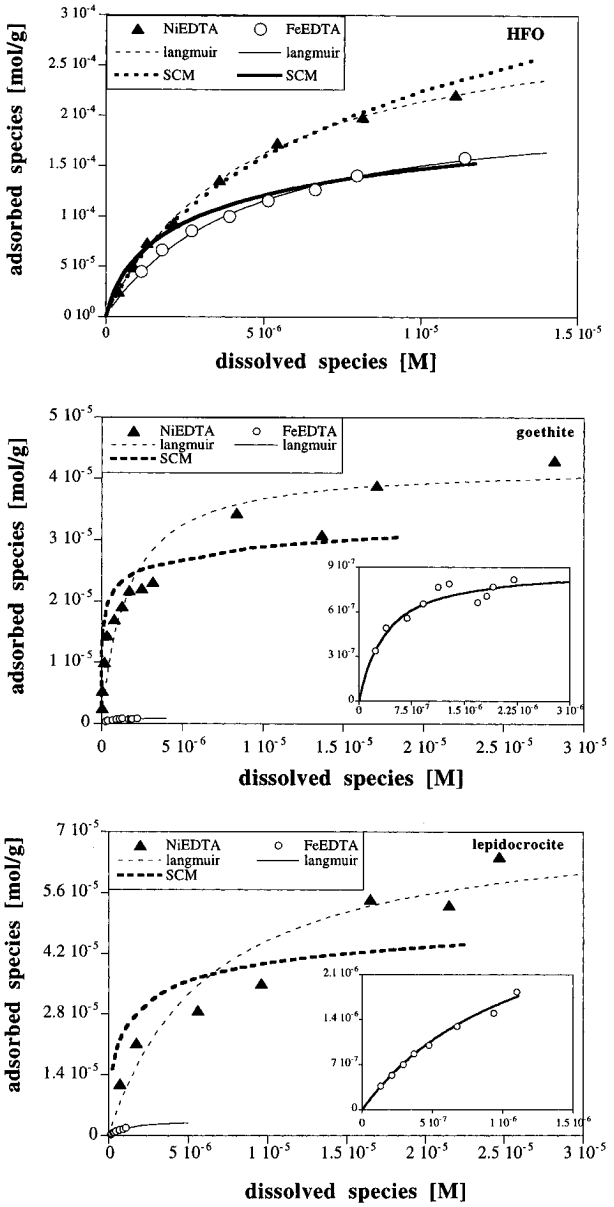

FIGURE 1. Adsorption isotherms of NiEDTA and Fe(III)EDTA onto the iron oxides goethite and lepidocrocite at pH 3.3 and HFO at pH 5.5. The data are calculated according to the Langmuir equation, eq 4, and the surface complexation model (SCM). The inset shows the enlarged adsorption isotherms of FeEDTA. Conditions for NiEDTA: HFO 0.08, goethite 0.12, and lepidocrocite 0.14 g/L; for FeEDTA: HFO 0.08, goethite 1.7, and lepidocrocite 0.9 g/L; all experiments in 0.01 M $NaNO_3$. The lines are calculated with the estimated constants from Tables 3 (Langmuir), 4 (NiEDTA, SCM), and 7 (FeEDTA, SCM).

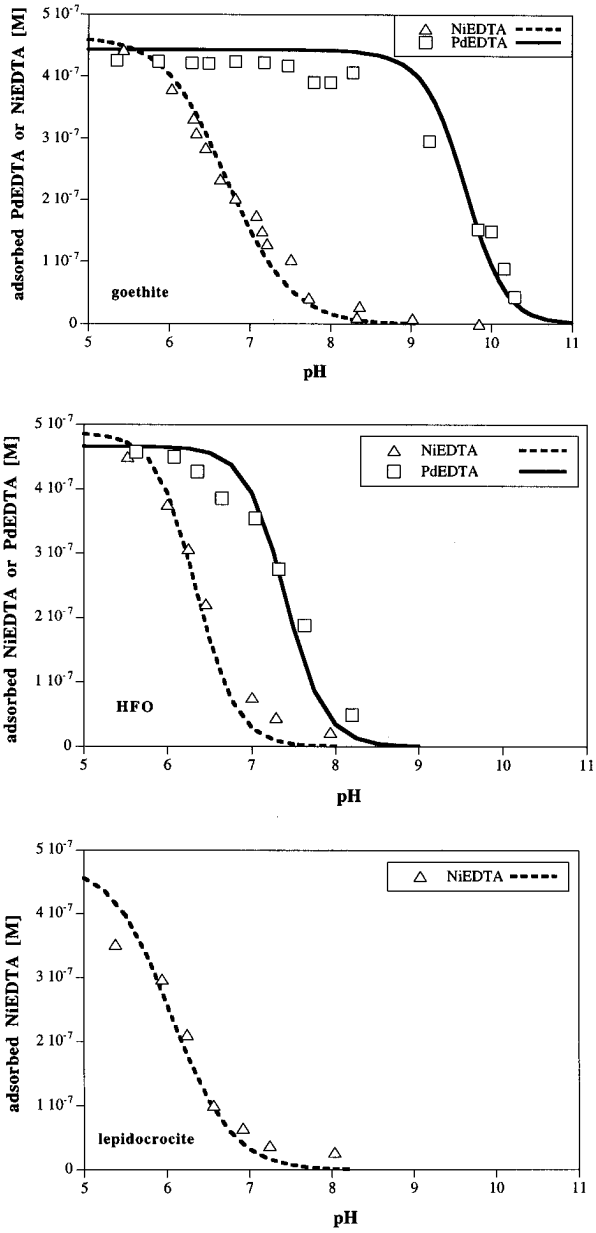

FIGURE 2. Adsorption edges of NiEDTA and PdEDTA onto the iron oxides goethite (0.46 g/L), HFO (0.08 g/L), and lepidocrocite (0.46 g/L). NiEDTA and PdEDTA 4.6×10^{-7} M, 0.01 M $NaNO_3$. The lines are calculated with the constants from Tables 4 and 6.

surface sites) are shown for these oxides. The adsorption edges vary by 2 pH units.

Adsorption of Me^{2+}EDTA other than NiEDTA. As reported previously, the complexes of small divalent metals [Ca, Zn, Cu, Co(II), Pb] adsorb in the same way (*15*, *16*). The data of Bowers and Huang (*15*) for the sorption of various Me^{2+}−EDTA complexes on aluminum oxides (*15*) gave log *K* values that agree very well when fitted by our model (Table 6). Complexes that have the same structure in solution exhibit the same adsorption behavior (*16*). Therefore, the EDTA complexes of Zn, Cu, Co(II), and Ca should have the same log *K* as NiEDTA with one oxide. With the exception of CaEDTA, where simultaneous adsorption of CaEDTA and uncomplexed EDTA onto goethite occurs, the log *K* values agree very well for the different complexes, both for goethite and for δ-Al_2O_3.

We were also able to fit the data of Girvin et al. (*17*) according to our model. The agreement between their experimental data for Co(II)EDTA and the model is very good (Figure 6). The pH_{50} values for Co(II)EDTA for this δ-Al_2O_3 is 8.4, which is higher than observed for all other oxides.

As reported by Nowack and Sigg (*16*), PdEDTA adsorbs very strongly to the goethite surface. For HFO, it was found that PdEDTA adsorption is also stronger than those of the other divalent metals. The adsorption edge can also be explained by a 1:1 surface complex. Model fits and experimental data for PdEDTA are also shown in Figure 2. Adsorption of PdEDTA to HFO is much weaker than to goethite, the log *K* values differ by 4 units. The adsorption well above the pzc indicates the formation of a specific surface complex.

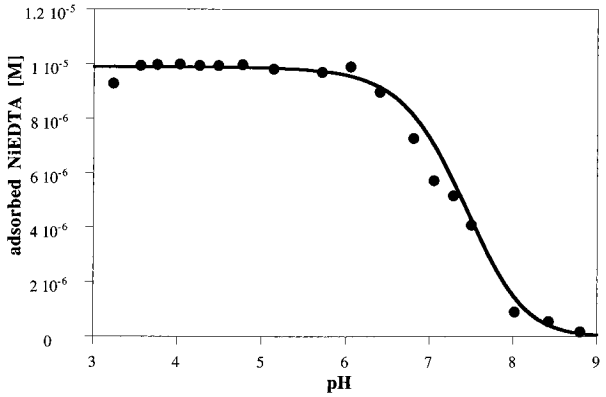

FIGURE 3. Adsorption edge of NiEDTA onto γ-Al_2O_3, data from Bowers (*10*). Oxide 1 g/L, NiEDTA 10^{-5} M, 0.025 M $NaClO_4$. The line was calculated with the constant from Table 4.

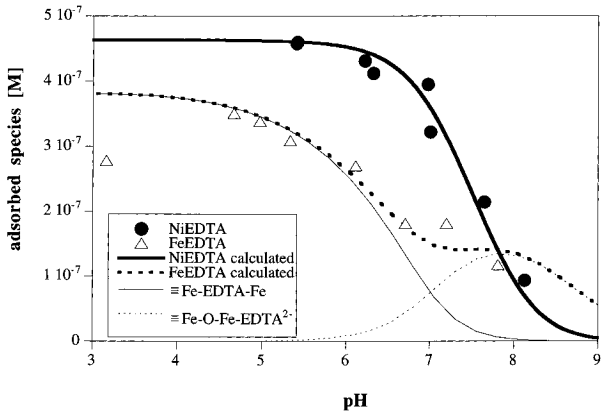

FIGURE 4. Adsorption edges of NiEDTA and Fe(III)EDTA onto δ-Al_2O_3 (0.46 g/L). Fe(III)EDTA 4.6×10^{-7} M, 0.01 M $NaNO_3$. The lines were calculated with the constants from Tables 4 and 7.

TABLE 5

pH of 50% Adsorption for Different Oxides and Different MeEDTA Complexes[a]

oxide	oxide concn (g/L)	species	pH_{50}	ref
HFO	0.44	NiEDTA	6.5	this study
HFO	0.44	NiEDTA	6.6	14
goethite	12.58	NiEDTA	8.1	16
lepidocrocite	9.16	NiEDTA	7.3	this study
δ-Al_2O_3	3.125	NiEDTA	8.4	this study
γ-Al_2O_3	6.25	NiEDTA	7.5	15
δ-Al_2O_3	6.25	Co(II)EDTA	8.1	17
goethite	12.58	Co(II)EDTA	8.0	16

[a] MeEDTA: 10^{-6} M; surface sites: 10^{-3} M.

Adsorption of Me^{3+}−EDTA. (a) Co(III)EDTA and AlEDTA. It was shown by Girvin et al. (*17*) that Co(III)-EDTA does not adsorb as strongly as Co(II)EDTA. Adsorption of Co(III)EDTA was explained by the following outer-sphere complex (*17*):

$$\equiv AlOH + Co(III)L^- + H^+ = \equiv AlOH_2^+ \text{---} {}^-LCo(III) \qquad (6)$$

An outer-sphere complex was assumed because in the Co-(III)EDTA complex all carboxylate groups are coordinated to the metal center whereas in the case of Co(II)EDTA one carboxylate group is free to coordinate with the surface (*16, 17*). Experimental data for the adsorption of Co(II)-EDTA and Co(III)EDTA onto δ-Al_2O_3 are shown in Figure 6 (from ref 17).

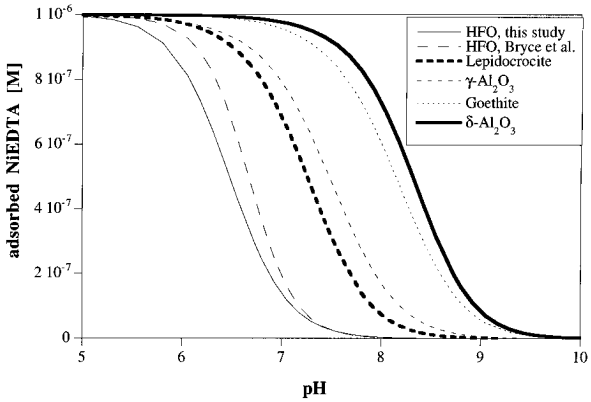

FIGURE 5. Adsorption edges of NiEDTA to several oxides for 1×10^{-6} M NiEDTA and 1 mM surface groups. The curves are calculated with the constants from Table 4.

TABLE 6

Intrinsic Log *K* Values for Adsorption of MeEDTA to Oxides ($I = 0$ M) for Reaction $\equiv SOH + MeL^{2-} + H^+ \Leftrightarrow \equiv S-L-Me^- + H_2O$, Model Constant Capacitance

species	HFO this study	goethite (*16*)	γ-Al_2O_3 (*17*)	δ-Al_2O_3 (*15*)
Ni	9.36	11.26	10.44[a]	11.55
Ca		12.26		11.09
Cu		11.44		11.08
Pb		11.18		11.03
Zn		10.85		11.01
Cd				11.54
Co(II)		11.05	11.97	
Pd	11.32	15.26		

[a] This study.

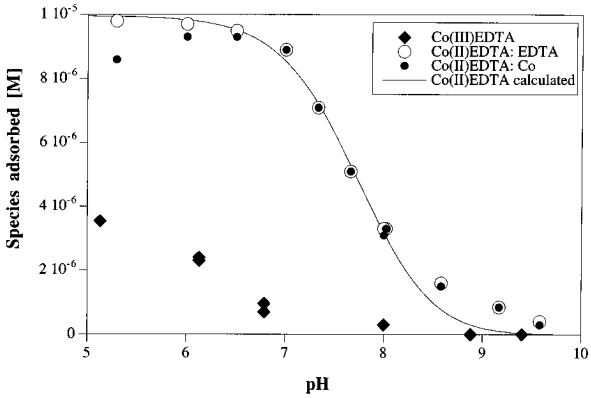

FIGURE 6. Adsorption edges of Co(III)EDTA and Co(II)EDTA onto δ-Al_2O_3, data from Girvin et al. (*17*). Oxide 1 g/L, MeEDTA 10^{-5} M, 0.01 M $NaClO_4$. The lines are calculated with the constants from Table 6.

AlEDTA exhibits a weaker adsorption on goethite than Me^{2+}−EDTA, but stronger than Co(III)EDTA (*16*). The adsorption edge onto goethite can be explained by taking into account: (i) adsorption of AlEDTA assuming the same log *K* as Co(III)EDTA. AlEDTA has a structure similar to Co(III)EDTA, which is sexidentate, and AlEDTA may also be sexidentate at pH 8 (*32*). AlEDTA and Co(III)EDTA should therefore have the same adsorption behavior (*16*). (ii) adsorption of uncomplexed EDTA (*16*). (iii) complexation of EDTA and Al^{3+} with H^+ and OH^- in aqueous solution.

With these assumptions, the adsorption of EDTA in the Al−EDTA−goethite system can be calculated. The result

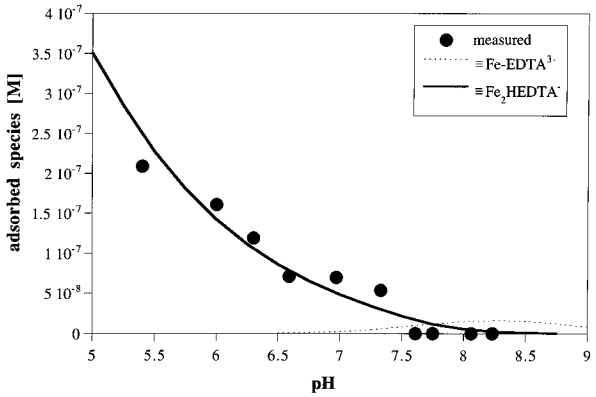

FIGURE 7. Adsorption edge of EDTA in the system EDTA−Al−goethite. Goethite 0.46 g/L, AlEDTA 4.6 × 10^{-7} M, 0.01 M $NaNO_3$. The lines are calculated with the log *K* values for the adsorption of uncomplexed EDTA to goethite from Nowack and Sigg (*16*). At low pH, a binuclear surface complex is assumed; at higher pH, a mononuclear surface complex is assumed.

is that no AlEDTA is adsorbed and that the surface species are ≡Fe−EDTA and ≡Fe_2−EDTAH (*16*). It is important to note that the curves in Figure 7 are calculated without fitting by using constants that are taken from the literature. The speciation of EDTA and Al is only valid for short equilibration times since dissolution of Fe(III) takes place at longer times. The subsequent formation and adsorption of Fe(III)EDTA alters the shape of the adsorption edge. The same dissociation and adsorption of uncomplexed EDTA was shown to occur with CaEDTA at low pH (*16*). If the same calculation is made for stronger EDTA complexes like Co(II)EDTA or NiEDTA, no dissociation and adsorption of uncomplexed EDTA is observed.

(b) Fe(III)EDTA. Fe(III)EDTA shows unusual adsorption behavior with strong adsorption in the high pH range, particularly by goethite and HFO. This behavior cannot be explained by one surface complex and must be due to an overlapping of two or more different surface complexes. For goethite, it was assumed by Nowack and Sigg (*16*) that two complexes, ≡Fe−EDTA−Fe^0 and ≡FeO−Fe−$EDTA^{2-}$, are formed. With these two complexes, the HFO and lepidocrocite data can also be explained very well.

The reactions used for modeling the Fe(III)EDTA adsorption are the following:

$$\equiv FeOH + FeEDTA^- + H^+ \leftrightarrow \equiv Fe-EDTA-Fe^0 + H_2O \quad (7)$$

$$\equiv FeOH + FeEDTA^- + OH^- \leftrightarrow \equiv Fe-O-FeEDTA^{2-} + H_2O \quad (8)$$

Reaction 7, in which EDTA bridges between surface and the iron center, represents an anion-like surface complex. By analogy, reaction 8, in which iron bridges between surface and EDTA, represents a cation-like surface complex.

The FeEDTA adsorption isotherm for HFO at pH 3.3 shows an adsorption density Γ_{max} that is 45% of the one for NiEDTA (Table 3). For goethite and lepidocrocite at the same pH, Γ_{max} is only 2% and 5%, respectively (Figure 1). Fe(III)EDTA seems to bind only to a small amount of surface groups. For these oxides, the concentration of ≡$FeOH_{spec}$ is a very important parameter for the fitting by the surface complexation model.

In Figure 8, measured and calculated adsorption edges are shown for the three different iron oxides. The cationic

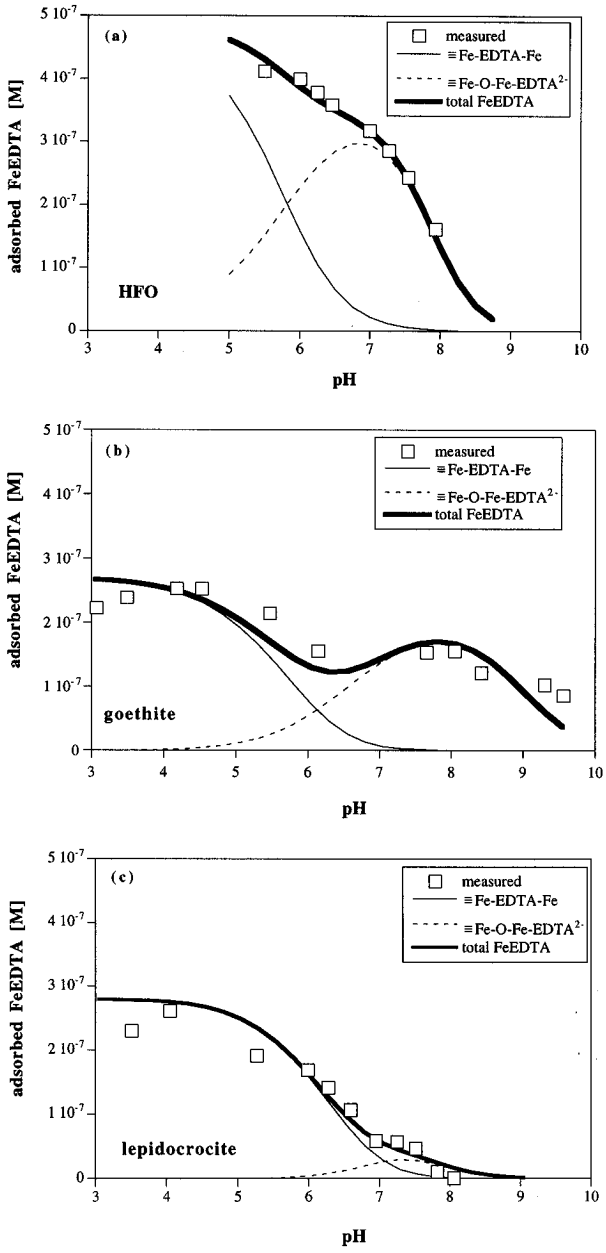

FIGURE 8. Adsorption edges of Fe(III)EDTA onto iron oxides: (a) HFO, 0.08 g/L, Fe(III)EDTA 4.6 × 10^{-7} M; (b) goethite 0.69 g/L, Fe(III)EDTA 6.9 × 10^{-7} M; (c) lepidocrocite 0.46 g/L, Fe(III)EDTA 4.6 × 10^{-7} M, all in 0.01 M $NaNO_3$. The lines are calculated with the constants from Table 7.

complex is very important for HFO and goethite, while for lepidocrocite it is nearly insignificant. The log *K* values are summarized in Table 7. If adsorption isotherms at constant pH are fitted, the amount of specific surface sites ≡$FeOH_{spec}$ has a great influence on the log *K* value. To obtain a reliable set of constants for FeEDTA, the model has to be improved and more measurements have to be made. Only for HFO with the highest Γ_{max} for FeEDTA, a log *K* value for an adsorption isotherm is given in Table 7, data and model fits are shown in Figure 1a.

To discern if adsorption of Fe(III)EDTA to an iron oxide is governed by adsorption of the complexed iron to the iron oxide surface, thus reacting similar to crystal growth, we also investigated the adsorption of Fe(III)EDTA to an aluminium oxide. We found the same adsorption behavior as for iron oxides, where Fe(III)EDTA adsorption is slightly weaker than the NiEDTA adsorption (Figure 4). This shows

TABLE 7

Intrinsic Log K Values for Adsorption of FeEDTA to Oxides (I = 0 M) for Reactions $\equiv FeOH + L^- + H^+ \leftrightarrow \equiv Fe-L-Fe^0 + H_2O$ (log K_1) and $\equiv FeOH + FeL^- + OH^- \leftrightarrow \equiv Fe-O-FeL^{2-} + H_2O$ (log K_2)

oxide	log K_1 $\equiv Fe-L-Fe^0$	log K_2 $\equiv Fe-O-Fe-L^{2-}$	error estimate SOS/DF	experiment
HFO	10.97 ± 0.30	−1.44 ± 0.07	0.12	pH edge
HFO	10.04 ± 0.32	−0.81 ± 0.14	8.37	a.i. pH 5.40[a]
goethite	12.26 ± 0.11	−0.42 ± 0.06	13.6	pH edge
lepidocrocite	12.62 ± 0.06	−1.16 ± 0.12	4.22	pH edge
δ-Al_2O_3	13.08 ± 0.15	−0.95 ± 0.14	2.07	pH edge

[a] a.i., adsorption isotherm at given pH.

that Fe(III)EDTA reacts at the aluminium oxide surface in the same way as on the iron oxide surface. The adsorption edge can be modeled with the same two surface complexes as for the iron oxides. The log K values (Table 7) are in the same range as the other values.

The adsorption of FeEDTA at high pH is due to the adsorption of FeEDTA as a complex. A dissociation and adsorption of uncomplexed EDTA and Fe onto different surface sites cannot explain the adsorption edge, because uncomplexed EDTA alone shows a weaker adsorption than FeEDTA. At pH 8.5, where the adsorption of FeEDTA onto goethite is still significant, adsorption of uncomplexed EDTA is very weak (*16*). It is also possible to desorb FeEDTA by competition with phosphate and to measure both Fe and EDTA again in solution. Adsorbed Fe(III) cannot be desorbed by phosphate at pH 7. The reversibility of the process indicates therefore the adsorption of the entire complex.

Discussion

The advantages of using a simple model for the description of adsorption data were demonstrated convincingly by Dzombak and Morel (*21*). Their work provides a consistent data base for the adsorption of anions and cations onto HFO. Due to the formulation of mean pK_a values for all HFO, the parameters (i.e., intrinsic adsorption constants) are directly comparable.

We show that it is also possible to model the adsorption of MeEDTA complexes (Me = divalent cations) to several oxides by a very simple model. The agreement between experimental data and model calculations is good for all oxides and complexes. The influence of the description of the acid−base properties of the oxides was shown for NiEDTA. If no data for the sorbent titration are available, the application of data from the literature can change the adsorption constants due to the different pK_a values. This effect was shown for our HFO by calculating the adsorption constant for NiEDTA with both our own pK_a values and the best-estimated values of Dzombak and Morel (*21*). A comparison of different oxides with different pK_a values can be made by calculating pH_{50}, the pH where 50% of EDTA is adsorbed under the same conditions for all oxides (same MeEDTA and surface site concentration). Adsorption decreases in the order δ-Al_2O_3 > goethite > γ-Al_2O_3 > lepidocrocite > HFO (*14*) > HFO (this study). The HFO of Bryce et al. (*14*), who used the pK_a values from Dzombak and Morel (*21*), and the HFO from this study, with quite different pK_a values both gave the lowest pH_{50} of all. It appears that the protonation constants of the oxide have little influence on the adsorption behavior, although they significantly change the speciation of the surface groups. Another possibility is that the HFO of Bryce et al. (*14*) had similar surface properties as our HFO.

By using a simple model with only one type of surface complex, we are able to model the adsorption of Me^{2+}−EDTA. Because all the complexes of the small divalent metals have the same log K value, it is easy to determine the adsorption behavior to one particular oxide by investigating just the adsorption of a single complex. NiEDTA is the most suitable complex because the dissolution of the oxides by this component is very slow (*33*). Therefore, the adsorption process on iron oxides can be studied without interference of Fe(III) dissolution and subsequent FeEDTA formation and adsorption.

PdEDTA also adsorbs much stronger onto goethite than onto HFO. Under the conditions of Figure 2, the pH edge of PdEDTA in comparison to NiEDTA is shifted 4 pH units higher for goethite, whereas for HFO it is only about 1 pH unit (Figure 2). It is not clear what causes this great difference. The adsorption of PdEDTA to goethite is clearly anionic and can be compared to vanadate or arsenate (*21*).

The adsorption of Fe(III)EDTA onto iron oxides shows another behavior. Adsorption of this complex still occurs at pH values between 7 and 8. Two different surface complexes are necessary to fit the data. The difference between Γ_{max} of Fe(III)EDTA and NiEDTA for both goethite and HFO is significant. For goethite $(\Gamma_{max,\ NiEDTA})/(\Gamma_{max,\ FeEDTA})$ is 47, for HFO it is 2.2. A possible explanation is the binding of Fe(III)EDTA to only one type of surface sites, which is more abundant on HFO than on goethite. Our modeling assumed therefore that FeEDTA binds only to specific surface groups. Spadini et al. (*34*) pointed out that HFO and goethite have a similar local structure but that they differ from lepidocrocite. The relative distribution of O and OH groups around Fe atoms is the same on HFO and goethite. Due to this fact, goethite and HFO should behave in the same way whereas lepidocrocite should behave differently. But Spadini et al. (*34*) also pointed out that HFO and goethite differ by the amount of high-affinity free edge sites. Goethite with needle-shaped crystals has, compared to HFO with much shorter crystals, less high-energy edge sites per unit surface area. It can be hypothesized that Fe(III)EDTA binds favorably to these high-energy sites. HFO would then be able to bind much more FeEDTA than goethite per unit surface area. If these high-energy sites show a different acid−base behavior than the overall pK_a values (in our modeling the same pK_a values were taken for specific and proton-binding sites), it could also explain the particular shape of the pH edge.

Adsorption of Fe(III)EDTA does not follow the same simple process as the other complexes. It could be shown that several surface complexes are necessary to explain the observed adsorption edge and the adsorption isotherms. The assumed stoichiometry of the surface complexes is necessary within our model to fit the data. These surface complexes may not, however, have real chemical meaning, but may only be relevant for the purpose of modeling. The structure and the type of these surface complexes have to be investigated by surface spectroscopic methods, such as FTIR, Raman, or EXAFS, which would help us to identify them.

Above pH 7, Fe(III)EDTA is the most important adsorbing species, with the exception of some complexes of heavy metal ions like Pd or La and Bi (*16*). Fe(III)EDTA was found

to be an important species in the effluent from wastewater treatment plants and in rivers (*4*). At lower pH, Fe(III)-EDTA is also formed by dissolution of iron oxides with metal−EDTA complexes (*1*, *2*). Due to adsorption even at pH 8, Fe(III)EDTA may be of significant importance in the adsorption of EDTA onto natural particles. For the possible scavenging of EDTA in lakes at pH 8 (*6*), the fraction of EDTA as Fe(III)EDTA may be the key parameter. In this case, Fe(III)EDTA would be adsorbed to settling particles whereas the other species would not react with surfaces.

Considering the adsorption of metal−EDTA species onto natural particles in lakes or rivers or onto aquifer material, we must therefore distinguish between the different complexes. Zobrist and Schönenberger (*35*), for example, have found in column experiments with a calcareous sand at pH 8 that Fe(III)EDTA exhibited a stronger retardation than CaEDTA or ZnEDTA and is thus in good agreement with our results. The differences in the strength of adsorption between different oxides has also to be considered. The adsorption edges for NiEDTA lie between pH 6 and pH 8, depending on the oxide, corresponding to the pH in natural aquifer systems. Retardation may therefore largely depend on the type of oxide present in these systems. Knowledge about concentration and nature of the reactive sites in aquifers, which are assumed to be mainly iron oxides (*36*, *37*), is therefore a major task in modeling the interactions of EDTA complexes with surfaces.

Acknowledgments

We thank John Westall for helpful comments, Hans-Ulrich Laubscher for the lepidocrocite, Daniel Kobler for the BET measurements, and Michael Elovitz for English corrections. The support of the Körber-Stiftung, Hamburg, Germany, and the French "Ministère de l'Environnement" (Grant DRAEI/92159) is acknowledged. J. L. is supported by CEC Grant 910959 STEP.

Literature Cited

(1) Kent, D. B.; Davis, J. A.; Anderson, L. D.; Rea, B. A. In *Water-Rock Interaction*; Kharaka, Y. K., Maest, A. S., Eds.; . A. A. Balkema: Rotterdam, Brookfield, 1992; pp 805−808.
(2) Szecsody, J. E.; Zachara, J. M.; Bruckhart, P. L. *Environ. Sci. Technol.* **1994**, *28*, 1706−1716.
(3) Kari, F. G.; Giger, W. *Water Res.* **1995**, *30*, 122−134.
(4) Kari, F. G.; Giger, W. *Environ. Sci. Technol.* **1995**, *29*, 2814−2827.
(5) Kari, F. G. Dissertation ETH No. 10698, Zürich, 1994.
(6) Ulrich, M. Dissertation ETH No. 9632, Zürich, 1991.
(7) *Ber. Int. Gewässerschutzkomm. Bodensee* **1991**, *41*.
(8) Bergers, P. J. M.; de Groot, A. C. *Water Res.* **1994**, *28*, 639−642.
(9) Toste, A. P.; Osborn, B. C.; Polach, K. J.; Lechner-Fish, T. J. *J. Radioanal. Nucl. Chem.* **1995**, *194*, 25−34.
(10) Bowers, A. R. Ph.D. Thesis, University of Delaware, 1982.
(11) Bowers, A. R.; Huang, C. P. *J. Colloid Interface Sci.* **1985**, *105*, 197−215.
(12) Blesa, M. A.; Borghi, E. B.; Maroto, A. J. G.; Regazzoni, A. E. *J. Colloid Interface Sci.* **1984**, *98*, 295−305 .
(13) Xue, H.; Kari, F. G.; Sigg, L. *Environ. Sci. Technol.* **1995**, *29*, 59−68.
(14) Bryce, A. L.; Kornicker, W. A.; Elzermann, A. W.; Clark, S. B. *Environ. Sci. Technol.* **1994**, *28*, 2353−2359.
(15) Bowers, A. R.; Huang, C. P. *J. Colloid Interface Sci.* **1986**, *110*, 575−590.
(16) Nowack, B.; Sigg, L. *J. Colloid Interface Sci.* **1996**, *177*, 106−121.
(17) Girvin, D. C.; Gassmann, P. L.; Bolton, H. *Soil Sci. Soc. Am. J.* **1993**, *57*, 47−57.
(18) Furrer, G.; Stumm, W. *Geochim. Cosmochim. Acta* **1986**, *50*, 1847−1860, .
(19) Zinder, B.; Furrer, G.; Stumm, W. *Geochim. Cosmochim. Acta* **1986**, *50*, 1861−1869.
(20) Nowack, B.; Sigg, L. *Environ. Sci. Technol.* **1995**, *29*, 3070−3071.
(21) Dzombak, D. A.; Morel, F. M. M. *Surface complexation modeling*; John Wiley and Sons: New York, 1990.
(22) Schwertmann, U.; Cornell, R. M. *Iron Oxides in the Laboratory*; VCH: Basel, 1991.
(23) Karametaxas, G.; Hug, S.; Sulzberger, B. *Environ. Sci. Technol.* **1995**, *29*, 2992−3000.
(24) Ochs, M. Dissertation ETH No. 9571, Zürich, 1991.
(25) Xue, H. B.; Sigg, L. *Anal. Chim. Acta* **1994**, *284*, 505−515.
(26) Good, N. E.; Winget, G. D.; Winter, W.; Conolly, T. N.; Izawa, S.; Raizada, M. M. *Biochemistry* **1966**, *5*, 467.
(27) Westall, J. C. *FITEQL: A program for the determination of chemical equilibrium constants from experimental data*; Technical Report; Chemistry Department, Oregon State University: Corvallis, OR, 1982.
(28) Kehrer, K. P. Thesis, University of Delaware, 1984.
(29) Kanungo, S. B. *J. Colloid Interface Sci.* **1994**, *162*, 86−92.
(30) Van den Berg, C. M. G.; Kramer, J. R. *Anal. Chim. Acta* **1979**, *106*, 13−120.
(31) Tiffreau, Ch.; Lützenkirchen, J.; Behra, Ph. *J. Colloid Interface Sci.* **1995**, *172*, 82−93.
(32) Howarth, O. W.; Moore, P.; Winterton, N. *J. Chem. Soc. Dalton Trans.* **1974**, 2271−2276.
(33) Nowack, B.; Sigg, L. Submitted for publication in *Geochim. Cosmochim. Acta*.
(34) Spadini, L.; Manceau, A.; Schindler, P. W.; Charlet, L. *J. Colloid Interface Sci.* **1994**, *168* 73−86.
(35) Zobrist, J.; Schönenberger, R. Manuscript in prep.
(36) Davis, J. A.; Kent, D. B.; Rea, B. A.; Maest, A. S.; Garabedian, S. P. In *Metals in Groundwater*; Allen, M. E., Perdue, E. M., Brown, D. S., Eds.; Lewis Publishers: Chelsea, MI, 1993; 223-273.
(37) Behra, Ph. Ph.D. Thesis, Université Louis Pasteur, Strasbourg, 1987.

Received for review November 29, 1995. Revised manuscript received March 1, 1996. Accepted March 6, 1996.[⊗]

ES9508939

[⊗] Abstract published in *Advance ACS Abstracts*, May 1, 1996.